

Inter-Aromatic Distances in *Geobacter Sulfurreducens* Pili Relevant to Biofilm Charge Transport

Hengjing Yan, Chern Chuang, Andriy Zhugayevych, Sergei Tretiak,*
Frederick W. Dahlquist,* and Guillermo C. Bazan*

Biological films containing the microbe *Geobacter sulfurreducens*, as well as protein layers composed of pili filaments, have been recently reported to exhibit electrical conductivities similar to those of doped organic semiconductors.^[1,2] The temperature dependence of these conductivities has led to lively debate on the most appropriate transport mechanisms: “electron hopping” or “metallic conduction.” One line of thinking proposes that charge equivalents are conducted on pili by a succession of electron transfer reactions among redox proteins.^[3,4] An opposing view provides the idea that the pili have metallic conductivity and invokes π - π interchain stacking between aromatic amino acid residues as the critical electron-coupling unit for charge transport.^[2,5] Difficulties in purifying pili crystals and identifying the distances between extracellular cytochromes on pili^[6,7] prevent the correlation of the electrical properties to an assembled electroactive unit; clear structure-to-property relationships at the molecular level thus remain lacking.

In the area of molecular crystalline organic semiconductors one can find literature precedent of charge-carrier mobilities that can be described by either “band-like”^[8,9] or “hopping” transport regimes.^[10,11] Heavily doped π -conjugated polymers may also show “metallic” transport with conductivities above 100 S cm^{-1} .^[12] In both cases the necessary requirement for sustaining efficient charge transport is the existence of π - π couplings with strength ranging from tens of meV for

intermolecular electron transfer, to more than an eV for charge transport along a chain.^[13] This need for robust electronic communication between subunits imposes strict requirements on the intermolecular distances and orientations.^[14] Pentacene, for example, crystallizes in a layered structure and electronic structure calculations show that both interplanar distances and the tilting of the molecules can affect charge transport depending on the crystal polymorph.^[15–17]

Our aim in this contribution is to approach the problem of charge-carrier conduction in *G. sulfurreducens* pili (GS pili) from the perspective of what is known on organic semiconducting materials. We will focus specifically on the conventional charge transport between aromatic units within the protein framework(s). These studies are relevant within the context of ongoing discussions on the extent to which this protein framework is capable of carrier transport in the absence of cytochromes.^[3–5] As described in more detail below, we first generated two GS pili subunit (pilin) models by using either homology considerations or nuclear magnetic resonance (NMR) spectroscopy characterization available in the literature.^[18,19] These two pilin structures were then used to build corresponding pili models. Inter-aromatic distances and orientations within two pili models were extracted to establish and evaluate electronic π - π couplings between aromatic residues in the pili structure. Finally, electron and hole transfer rates and mobilities within GS pili structure without extracellular redox mediators were calculated based on the small polaron hopping model^[13,14] and compared to GS pili experimental data and traditional organic semiconductors.

As shown in **Figure 1**, the GS pilin structure shares considerable sequence similarity to *Neisseria gonorrhoeae* (NG) pilin, the subunit of another type IVa pili.^[19] By virtue of this similarity we combined the NG pilin model (**Figure 2a**) and the *G. sulfurreducens* pilin sequence in SWISSMODEL using the automatic modeling mode.^[20,21] The resulting homology model ($\text{GS}_{\text{Homology}}$) of GS pilin, namely the PilA protein, is provided in **Figure 2b**. We also adopted the existing PilA model of *G. sulfurreducens* pili obtained by solution state NMR spectroscopy^[18] to generate GS_{NMR} as shown in **Figure 2c**. We found both $\text{GS}_{\text{Homology}}$ and GS_{NMR} models have 40% conserved structure with the NG pilin model and high α -helical contents in N-terminal region (77% for $\text{GS}_{\text{Homology}}$ and 80% for GS_{NMR}). This high structural conservation of GS pilin with NG pilin led us to hypothesize that their assembly into pili structures would exhibit similar packing.

Based on the molecular 3D coordinates in $\text{GS}_{\text{Homology}}$ and GS_{NMR} , we extracted inter-aromatic distances by measuring the shortest distance between aromatic ring centers for each pair

Dr. H. Yan
Department of Chemistry and Biochemistry
Center for Polymers and Organic Solids
University of California at Santa Barbara
Santa Barbara, CA 93106, USA
C. Chuang, Dr. A. Zhugayevych, Dr. Sergei Tretiak
Theoretical Division, Los Alamos National Laboratory
Los Alamos, NM 87545, USA
E-mail: serg@lanl.gov
Prof. F. W. Dahlquist
Department of Chemistry and Biochemistry
Department of Molecular
Cellular, and Developmental Biology
University of California at Santa Barbara
Santa Barbara, CA 93106, USA
E-mail: dahlquist@chem.ucsb.edu
Prof. G. C. Bazan
Department of Chemistry and Biochemistry
Department of Materials
Center for Polymers and Organic Solids
University of California at Santa Barbara
Santa Barbara, CA 93106, USA
E-mail: bazan@chem.ucsb.edu



DOI: 10.1002/adma.201404167

GS _{NMR}	1-35	FTLIELLIVVAIIGILAAIAIPQFSAYRVKAYNSA
GS _{Homology}	1-35	FTLIELLIVVAIIGILAAIAIPQFSAYRVKAYNSA
NG	1-35	FTLIELMIVIAIVGILAAVALPAYQDYTARAQVSE
Conservation		*****
GS _{NMR}	36-70	ASSDLRNLKTALESAFADDQTYPPES-----
GS _{Homology}	36-70	ASSDLRNLKTALESAFADDQTYPPES-----
NG	36-70	AILLAEQKSAVTEYYLNHGKWPENNTSAGVASSP
Conservation		***

Figure 1. Alignment of amino acid sequences from two GS pilin models with the amino acid sequence from *N. gonorrhoeae* pilin (truncated to 70 amino acids). Aromatic residues (red), residues in helical structure (yellow background), and conserved residue (with * and purple background in the bottom row) are highlighted.

of aromatic residues in GS pilin (same for subsequent analysis), which are phenylalanine and tyrosine. Inter-aromatic distances within a single pilin monomer exhibit a wide range, from 6.5 to 35.6 Å. These distances, particularly the larger values, are considerably longer than those typical of high mobility organic semiconducting or conducting materials, and immediately argue against a similar transport mechanism. We thus examined other possible contacts as a result of inter-pilin packing in the pilin superstructure.

The regions of high sequence conservation between NG and GS pilin are largely responsible for the assembly of the pilus filament in the filament model proposed by the Tainer laboratory from a combination of X-ray and cryoelectron tomography.^[19] We thus modeled the assembly in analogy to *N. gonorrhoeae* pilin (NG pilin), by aligning each GS pilin to NG pilin in PyMol.^[19,22] In our approach, the GS pilins were brought together and projected against the previously characterized NG pilin structure.^[23] As is the case with NG pilin, both GS_{NMR} pilin and GS_{Homology} pilin models exhibit helical arrangements within the GS pilin superstructure (Figure 3). The diameter of the GS pilin in our model ranged from 36.5 to 58 Å, which is consistent with experimental values observed from atomic force microscopy.^[2] In the

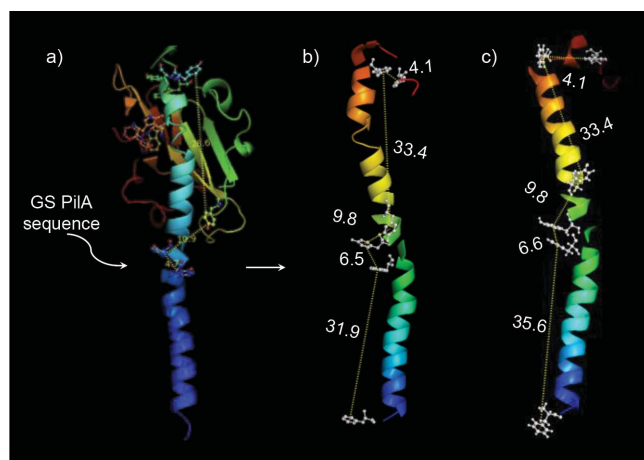


Figure 2. a) *N. gonorrhoeae* pilin model used for building b) *G. sulfurreducens* pilin homology model. c) Another GS pilin model based on NMR spectroscopy results is also adopted in this study. Aromatic residues are shown as stick and ball and the rest are shown in cartoon representation. Inter-aromatic distances (Å) are labeled beside the two GS pilin models.

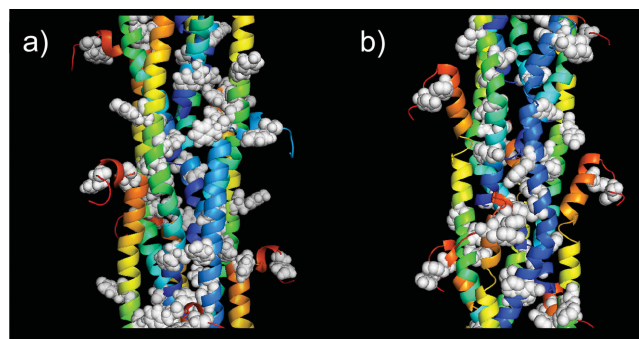


Figure 3. a) The GS_{NMR} pilin model built from the GS_{NMR} pilin model and NG pilin model. b) The GS_{Homology} pilin model built from GS_{Homology} pilin model and NG pilin model. Aromatic residues are shown as white spheres and the rest are shown as a rainbow colored cartoon.

GS_{NMR} pilin model, phenylalanine-24, tyrosine-27 and phenylalanine-51 are found clustered in the inner space of the pilin with inter-aromatic distances of 6.6, 10.4, and 8.6 Å (Figure 4). Those three residues from each monomer formed a tentative helical pathway for electron hopping. In the GS_{Homology} pilin model, a similar helical pathway of phenylalanine-24 and tyrosine-27 with inter-aromatic distances of 6.5 and 10.8 Å can be identified, see Figure S1, Supporting Information. However, since phenylalanine-51 in both GS_{Homology} and GS_{NMR} pilin models is located in the free head C-terminal region, its position is anticipated to be the least accurate due to its higher propensity to perturbations by the environment.

The molecular details of the two pilin models were incorporated into our calculation of electronic structure. A more quantitative evaluation of charge transport properties was accomplished through the application of modeling proven for organic semiconductors. Full technical details of these calculations are given in Supporting Information; we focus here on the principal approach and relevant conclusions. We first computed the electronic properties of the hydrogen-passivated aromatic residues in their actual spatial location. The rest of the protein is modeled as a continuum polarizable medium with the dielectric constant $\epsilon = 20$.^[23] The electronic couplings between the π -conjugated fragments are estimated within the dimer

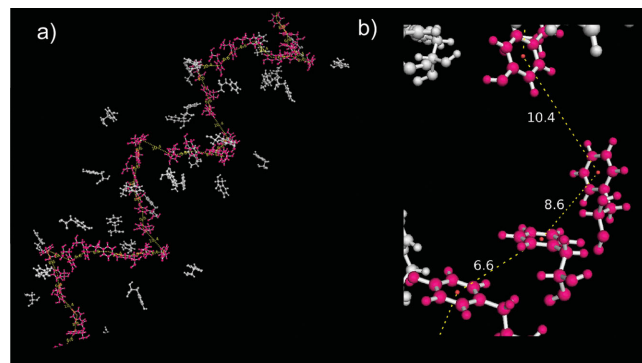


Figure 4. a) Aromatic residues (pink and white stick-and-balls) from GS_{NMR} are extracted. b) Zoomed-in inter-aromatic distances (Å) indicate a helical pathway through identical aromatic residues (in pink) for longitudinal charge transport within pilin.

Table 1. Summary of charge transport properties of GS_{Homology} and GS_{NMR} pili models and experimental values of GS pili and pentacene.

Charge carrier	GS _{Homology}		GS _{NMR}		GS pili	Pentacene
	Hole	Electron	Hole	Electron	Exp value	Exp value
Inverse rate [ps]	7.7×10^{14}	1.2×10^{16}	1.1×10^{13}	9.1×10^{12}	N.A.	N.A.
Diffusion coefficient [cm ² s ⁻¹]	1.4×10^{-17}	9.4×10^{-19}	1.0×10^{-15}	1.2×10^{-15}	N.A.	N.A.
Charge mobility [cm ² V ⁻¹ s ⁻¹]	5.6×10^{-16}	3.3×10^{-17}	3.9×10^{-14}	4.7×10^{-14}	N.A.	0.1 to 0.5 ^{b)}
Conductivity [μ S cm ⁻¹]	1.4×10^{-8}		2.0×10^{-6}		6 ^{a)}	N.A.

^{a)}The conductivity of GS pili filament preparation obtained in experiment,^[2] where the presence of extracellular cytochromes in the preparation is under debate;^[3,4] ^{b)}The charge mobility of pentacene single crystal obtained in experiment.^[28]

approximation using density functional theory with CAM-B3LYP functional^[24] and 6–31G basis set.^[25,26] Thus obtained values do not exceed a few meV, except for isolated pairs. Such minimal interactions suggest the charge-carrier transport regime to be hopping. Inter-fragment transfer rates depend strongly on the reaction transfer energies, ΔG° , which themselves are highly sensitive to the environment. This uncertainty disappears if we are interested only in the upper limit of the transfer rates, which can be reliably estimated by the prefactor of the Marcus formula:^[27]

$$w \leq t^2 \sqrt{\frac{\pi}{\hbar^2 \lambda k T}} \quad (1)$$

where t is the electronic coupling and λ is the charge transfer reorganization energy, which is about 0.4 eV for all the residues (intramolecular contribution). For these rates, the dominant charge transfer routes are shown by the inter-aromatic pathways such as that in Figure 4 and Figure S1, Supporting Information. The lowest transfer rates along these routes are on the scale of inverse seconds, dramatically slowing down the electronic transport. As a result, the calculated electron (μ_e) and hole (μ_h) mobilities do not exceed 10^{-14} cm² V⁻¹ s⁻¹ for both GS_{Homology} and GS_{NMR} pili models (Table 1), which is at least 13 magnitudes smaller than single crystal pentacene.^[28] Under these conditions and by using the relationship between conductivity (σ), mobility, and carrier concentration (ρ), i.e., $\sigma = \rho(\mu_h + \mu_e)$, and using the number density of aromatic residues as the maximum value of ρ leads to σ values of 1.4×10^{-8} μ S cm⁻¹ and 2×10^{-6} μ S cm⁻¹ for GS_{Homology} and GS_{NMR} pili structures, respectively, compared to the conductivity of GS pili obtained in previous experiment study, i.e., 6 μ S cm⁻¹.^[2] Even if errors of calculation in conductivities reach to two to three orders of magnitude due to the fluctuations of contact distances in both models (Figure S2 and S3, Supporting Information), they are far below measured values.

We next examine dynamic processes that may impact electronic couplings. Specifically, we used a simplified approach to estimate how the upper limit of conductivity can be influenced by intermolecular (mainly via t) and environmental (mainly via ΔG°) fluctuations.^[27,29] Because the charge solvation energy for the aromatic residues (about 2 eV, see Table S2, Supporting Information) is much larger than λ and ΔG° (tenths of eV), the exponential factor in the Marcus formula is anticipated to fluctuate across a wide range. To remove this uncertainty we replaced it by its maximum value; i.e., unity, as in Equation (1).

Fluctuations of intermolecular geometry were modeled by statistical sampling of random translations and rotations with the amplitude matching estimated Debye–Waller factors (DWFs).^[30] The upper limit for Equation (1) is given by replacing t^2 by its average value (fast-fluctuations limit).^[29] We recognize that the DWF approach may not fully describe bending and/or other temporary deformations within the overall superstructure; however, it is sufficient to explore upper limits of conductivity. The results showed that the deviation of contact distances between the rate-limiting pair fragments for proposed electron transfer in GS_{NMR} (i.e., tyrosine-27 and phenylalanine-51), matching the estimated DWF of about 30 Å² (Table S11, Supporting Information), will be less than 1 Å (Table S10, Supporting Information). The corresponding transfer integral is on average approximately $10^{-1.5}$ meV, with fluctuations ranging between 10^{-3} and $10^{-1.5}$ meV (Table S10 and Figure S2, Supporting Information). Under these conditions, and assuming the maximum of one charge carrier per aromatic residue, the conductivity can reach up to 100 μ S cm⁻¹. Achieving this value requires meeting multiple extraordinary conditions, including the maximum possible values for ρ , which is unphysical, and the exponential factor being unity in the Marcus formula. We can thus conclude that the interaromatic pathway is an unlikely mechanism of conductivity.^[14,31]

The work described here provides a perspective of the spatial location of aromatic units within GS pili superstructure based on an analogy to *N. gonorrhoeae* pili, as both share high sequence conservation regions in subunits responsible for superstructure assembly. Moreover, the general approach forms the basis for correlating protein structure with electrical properties. Using the ensemble of aromatic units within the protein as input for quantum mechanical electronic calculation methods leads to charge-carrier mobilities that are insufficient to account for experimentally determined conductivities. The low electronic transport is a consequence that aromatic amino acids are not packed sufficiently tight for π – π interactions. These results based on such a geometry are in contrast with highly cited mechanistic proposals for those biological films,^[2,5,6] which invoke inter-aromatic contacts as being critical to the conductivity measurements of biological films, thus paralleling the conductivity mechanisms of biological films with that in conducting conjugated materials. Additional factors that may be relevant to reconcile theoretical analysis and published experimental results include the influence of extracellular cytochromes,^[3,4] perturbations by virtue of ion conductivity, differences in pili aromatic content between GS and

N. gonorrhoeae, and protein conformations very far from the equilibrium structures used for calculations here. Despite these uncertainties, the methodology described here provides a potentially general method of correlating protein structure to electronic charge transport.

Supporting Information

Supporting Information is available from the Wiley Online Library or from the author.

Acknowledgements

Funding was provided by the Institute for Collaborative Biotechnologies (ICB) under Grant No. W911F-09-D-0001 from the U.S. Army Research Office. This work was partially supported by LANL LDRD program and the Center for Integrated Nanotechnologies, a U.S. Department of Energy, and the Office of Basic Energy Sciences user facility.

Received: September 9, 2014

Revised: November 17, 2014

Published online: January 21, 2015

- [1] P. Parisse, M. Passacantando, S. Picozzi, L. Ottaviano, *Org. Electron.* **2006**, *7*, 403.
- [2] N. S. Malvankar, M. Vargas, K. P. Nevin, A. E. Franks, C. Leang, B. C. Kim, K. Inoue, T. Mester, S. F. Covalla, J. P. Johnson, V. M. Rotello, M. T. Tuominen, D. R. Lovley, *Nat. Nanotechnol.* **2011**, *6*, 573.
- [3] S. M. Strycharz-Glaven, R. M. Snider, A. Guiseppi-Elie, L. M. Tender, *Energy Environ. Sci.* **2011**, *4*, 4366.
- [4] S. M. Strycharz-Glaven, L. M. Tender, *Energy Environ. Sci.* **2012**, *5*, 6250.
- [5] N. S. Malvankar, M. T. Tuominen, D. R. Lovley, *Energy Environ. Sci.* **2012**, *5*, 6247.
- [6] C. Leang, X. L. Qian, T. Mester, D. R. Lovley, *Appl. Environ. Microbiol.* **2010**, *76*, 4080.
- [7] T. Mehta, M. V. Coppi, S. E. Childers, D. R. Lovley, *Appl. Environ. Microbiol.* **2005**, *71*, 8634.
- [8] O. Ostroverkhova, D. G. Cooke, S. Shcherbyna, R. F. Egerton, F. A. Hegmann, R. R. Tykwinski, J. E. Anthony, *Phys. Rev. B.* **2005**, *71*, 035204.
- [9] K. P. Pernstich, B. Rossner, B. Batlogg, *Nat. Mater.* **2008**, *7*, 321.
- [10] H. Bassler, *Phys. Status Solidi B* **1993**, *175*, 15.
- [11] Y. Olivier, V. Lemaur, J. L. Bredas, J. Cornil, *J. Phys. Chem. A.* **2006**, *110*, 6356.
- [12] A. N. Aleshin, *Phys. Solid State* **2010**, *52*, 2307.
- [13] A. Zhugayevych, O. Postupna, R. C. Bakus li, G. C. Welch, G. C. Bazan, S. Tretiak, *J. Phys. Chem. C.* **2013**, *117*, 4920.
- [14] V. Coropceanu, J. Cornil, D. A. da Silva, Y. Olivier, R. Silbey, J. L. Bredas, *Chem. Rev.* **2007**, *107*, 926.
- [15] C. C. Mattheus, A. B. Dros, J. Baas, G. T. Oostergetel, A. Meetsma, J. L. de Boer, T. T. M. Palstra, *Synth. Met.* **2003**, *138*, 475.
- [16] R. C. Haddon, X. Chi, M. E. Itkis, J. E. Anthony, D. L. Eaton, T. Siegrist, C. C. Mattheus, T. T. M. Palstra, *J. Phys. Chem. B.* **2002**, *106*, 8288.
- [17] J. L. Bredas, J. P. Calbert, D. A. da Silva, J. Cornil, *Proc. Natl. Acad. Sci. USA* **2002**, *99*, 5804.
- [18] P. N. Reardon, K. T. Mueller, *J. Biol. Chem.* **2013**, *288*, 29260.
- [19] L. Craig, N. Volkmann, A. S. Arvai, M. E. Pique, M. Yeager, E. H. Egelman, J. A. Tainer, *Mol. Cell* **2006**, *23*, 651.
- [20] K. Arnold, L. Bordoli, J. Kopp, T. Schwede, *Bioinformatics* **2006**, *22*, 195.
- [21] L. Bordoli, F. Kiefer, K. Arnold, P. Benkert, J. Battey, T. Schwede, *Nat. Protoc.* **2009**, *4*, 1.
- [22] The PyMOL Molecular Graphics System, Version 1.5.0.4 Schrödinger, LLC.
- [23] L. Li, C. Li, Z. Zhang, E. Alexov, *J. Chem. Theory Comput.* **2013**, *9*, 2126.
- [24] T. Yanai, D. P. Tew, N. C. Handy, *Chem. Phys. Lett.* **2004**, *393*, 51.
- [25] R. Ditchfield, W. J. Hehre, J. A. Pople, *J. Chem. Phys.* **1971**, *54*, 724.
- [26] W. J. Hehre, R. Ditchfield, J. A. Pople, *J. Chem. Phys.* **1972**, *56*, 2257.
- [27] V. Rühle, A. Lukyanov, F. May, M. Schrader, T. Vehoff, J. Kirkpatrick, B. Baumeier, D. Andrienko, *J. Chem. Theory Comput.* **2011**, *7*, 3335.
- [28] J. Takeya, C. Goldmann, S. Haas, K. P. Pernstich, B. Ketterer, B. Batlogg, *J. Appl. Phys.* **2003**, *94*, 5800.
- [29] D. N. Beratan, S. S. Skourtis, I. A. Balabin, A. Balaeff, S. Keinan, R. Venkatramani, D. Q. Xiao, *Acc. Chem. Res.* **2009**, *42*, 1669.
- [30] L. Meinhold, J. C. Smith, *Biophys. J.* **2005**, *88*, 2554.
- [31] A. J. Heeger, *Rev. Modern Phys.* **2001**, *73*, 681.